0026-895X/95/020381-10$03.00/0

MOLECULAR PHARMACOLOGY, 47:381–390, 1995.

Time- and Voltage-Dependent Block of Delayed Rectifier Potassium Channels by Docosahexaenoic Acid

JON S. POLING, JOHN W. KARANIAN, NORMAN SALEM, JR., and STEFANO VICINI

Laboratory of Membrane Biochemistry and Biophysics, Division of Intramural Clinical and Biological Research, National Institute on Alcohol Abuse and Alcoholism, Rockville, Maryland 20852 (J.S.P., J.W.K., N.S.), and Department of Physiology and Biophysics, Georgetown University School of Medicine, Washington, D. C. 20007 (J.S.P., S.V.)

Received August 11, 1994; Accepted November 4, 1994

SUMMARY

Docosahexaenoic acid (22:6n3) acts at an extracellular site to produce a voltage- and time-dependent block of the delayed rectifier current (I_K) similar to that classically described for intracellularly applied quaternary ammonia compounds. In dissociated cells from the pineal gland, some long-chain polyunsaturated fatty acids reduced both late sustained (I_K) (for 22:6n3, IC_{50} = 2.5 ± 0.3 μM) and early transient (I_A) (IC_{50} = 2.0 ± 0.1 μM) components of potassium current when applied extracellularly, whereas the monounsaturate oleic acid had minimal efficacy. From comparisons of other related fatty acids, it was determined that there is a structural requirement for polyunsaturation to block I_K. In contrast, chain-elongated 22-carbon polyunsaturates acted similarly to their precursor 20-carbon fatty acids (arachidonic acid and eicosapentanoic acid). Block of I_K by 22:6n3 was accompanied by a dose-dependent acceleration of the current decay in both whole-cell and outside-out membrane patches, and 22:6n3 increased the macroscopic inactivation rate of I_A. The combined "eicosanoid" inhibitor eicosatetraenoic acid, when included in the patch pipette, did not antagonize the action of 22:6n3. Instead, eicosatetraenoic acid produced a direct block of I_K when applied extracellularly at high concentrations (25 μM). Analyses of voltage- and time-dependent block by 22:6n3 support the hypothesis that certain fatty acids directly interact with and preferentially block the open state of some potassium channels. We also describe an interaction between fatty acid block and zinc; 22:6n3 failed to block either I_A or I_K in the presence of zinc or cadmium, whereas extracellular calcium did not affect the response. These studies suggest a possible biological function for 22:6n3 in the nervous system, which may underlie its essential role during neural development.

The role of ω-3 (*n*-3) fatty acids in the function of the central nervous system remains largely unknown. Epidemiological studies, however, have indicated that populations with high dietary levels of *n*-3 fatty acids have a lowered incidence of heart disease and diabetes (1). Of the two major *n*-3 fatty acids, 22:6n3 and 20:5n3, 22:6n3 is an essential component of biological membranes in the nervous system (2, 3). Salem and Niebylski (4) have recently suggested that the biological role of *n*-3 fatty acids in the brain and retina is not related to the production or inhibition of 20:4n6 metabolites but, instead, a direct role in the regulation of membrane protein function has been postulated. The essential precursor fatty acids linoleic acid and linolenic acid are required in the diet, and their deficiency results in known clinical sequelae with significant correlation to neurological deficits (5, 6); 22:6n3, which may be consumed preformed or synthesized by the liver or brain from linolenic acid (7), is essential for the proper development and maintenance of the central nervous system (8). Moreover, 22:6n3 has been demonstrated to be selectively recycled by photoreceptor outer segments and synapses (9). However, at present little is known about the mechanisms underlying the biological functions of 22:6n3. For these reasons, the present study focuses on the effect of 22:6n3 on membrane excitability in a specific area of the central nervous system.

The pineal gland, a derivative of the embryonic diencephalon, was initially selected as the focus of this study because it has been previously determined to be the only central nervous system structure that possesses stereospecific lipoxygenase enzyme activity (10). Potassium currents have been previously described (11) for acutely dissociated cells of the adult rat pineal gland, using the whole-cell configuration of the patch-clamp technique. In addition, earlier experiments partially characterized the membrane properties of rat pinealocytes in primary culture (12). The aforementioned studies reported the

This work was supported in part by a National Institutes of Health Intramural Research Training Fellowship award to J.S.P.

ABBREVIATIONS: 22:6n3, docosahexaenoic acid; 20:5n3, eicosapentaenoic acid; 20:4n6, arachidonic acid; 18:1n9, oleic acid; ETYA, 5,8,11,14-eicosatetraenoic acid; I_K, delayed rectifier K^+ current; I_A, transient outward K^+ current; BAPTA, 1,2-bis(2-aminophenoxy)ethane-*N*,*N*,*N*′,*N*′-tetraacetic acid; HEPES, 4-(2-hydroxyethyl)-1-piperazineethanesulfonic acid; EtOH, ethyl alcohol; H-7, 1-(5-isoquinolinesulfonyl)-2-methylpiperazine; 4-AP, 4-aminopyridine; P450, cytochrome P450; PUFA, polyunsaturated fatty acid; TEA-Cl, tetraethylammonium chloride; TEA, tetraethylammonium; 22:5n3, docosapentaenoic acid; 22:3n6, docosatrienoic acid; 22:4n3, docosatetraenoic acid; I_H, hyperpolarization-activated inward current.

presence of sustained and transient components of outward K^+ current in pinealocytes.

Ion channel modulation by PUFAs has been reported to act by a diverse set of mechanisms, i.e., directly or indirectly and at extracellular or intracellular receptor sites (13–15). The majority of studies on K^+ channels have focused on the action of 20:4n6 and its enzymatic metabolites, the "eicosanoids." Conflicting reports have been published regarding voltage-gated K^+ currents, indicating either inhibition (16) or enhancement (17) by micromolar concentrations of 20:4n6. In the present study, we investigate the effects of 22:6n3 on both I_K and a fast I_A, compared with other structurally related fatty acids.

Materials and Methods

Cell culture. Pinealocytes were prepared from newborn (day 1) Sprague-Dawley rats with modifications of a previously described protocol (18). The pineal gland was mechanically dissociated under a dissecting stereomicroscope, and small tissue explants were plated on glass coverslips, which had been coated with poly-L-lysine (10 μg/ml; Sigma Chemical Co., St. Louis, MO), in four-welled multidishes (Nunc, Roskilde, Denmark). Cells grew from explants over the course of 1 week in culture. Studies were performed between 7 and 28 days *in vitro*. The cultures were maintained in a 6% CO_2 incubator at 37°, in basal Eagle's medium to which was added 10% fetal bovine serum (GIBCO, Grand Island, NY), 25 mM KCl, 2 mM glutamine (Sigma), and 100 μg/ml gentamicin (GIBCO). The incubation medium was replaced 48 hr after plating, and cytosine arabinofuranoside (1 μM; Sigma) was added to inhibit the replication of non-neuronal cells.

Electrophysiology. Pinealocytes in primary culture were voltage-clamped, using the patch-clamp technique (19), on the stage of an inverted microscope (Olympus CK2, Lake Success, New York) at room temperature (22–25°). Currents were monitored with either EPC-7 (List Electronics, Darmstadt, Germany) or Axopatch-1D (Axon Instruments, Foster City, CA) patch amplifiers. Recording electrodes of 3–6-MΩ open-tip resistance in bath solution were pulled (with a Narashige PP-83 pipette puller) from thin-walled glass micropipettes (Drummond Scientific, Broomall, PA). The recording electrode solution contained 140 mM KCl, 1 mM $MgCl_2$, 5 mM BAPTA, 2 mM NaATP, 0.2 mM NaGTP, and 10 mM HEPES, pH 7.2. The cells were bathed in 145 mM NaCl, 5 mM KCl, 1 mM $CaCl_2$, 1 mM $MgCl_2$, 5 mM glucose, 5 mM HEPES, pH 7.4; osmolarity was adjusted to 325 mOsM with sucrose. Nominally calcium-free extracellular solution used in some experiments contained 2 mM $MgCl_2$ and was otherwise the same. Phosphate-depleted intracellular solution was the same as described above, with the exception that no GTP or ATP was added.

Drugs and perfusion. The recording chamber (0.75-ml total volume) was continuously perfused at a rate of 3 ml/min. Fatty acids (NuCheck Prep, Elysian, MN) and ETYA (Calbiochem, San Diego, CA) were stored under N_2 at −70° in the dark, at a stock concentration of 0.1 M in EtOH, and were serially diluted in bath solution plus vehicle (0.1% EtOH) each day so that final concentrations ranged from 0.1 to 50 μM. Studies with 22:6n3 were also performed using solutions without 0.1% EtOH as a vehicle; no observable effect on the concentration-effect relationship was observed. In some experiments, the inhibitors ETYA, H-7, and staurosporine (Calbiochem) were added to the recording solutions. The P450 inhibitors metyrapone and SKF525-A (proadifen-HCl) were purchased from Biomol Research Laboratories (Plymouth Meeting, PA) and were added to recording solutions as indicated. In some experiments, 4-AP (5 mM; Sigma) and TEA-Cl (10 mM; Sigma) were added to the external bathing medium and the pH was corrected to 7.4. Fatty acids and/or vehicle were continuously applied using the Y-shaped tubing method (20). The Y-tubing applicator had a tip diameter of 150 μm and was positioned within 500 μm of the cell being investigated. With this method, a number of different test solutions could be applied and exchanged rapidly, with an onset of typically 1–2 msec. Onset time was measured from the open tip current induced by 10-fold diluted extracellular solution.

Data acquisition and analysis. Currents were filtered at 3 kHz with an eight-pole low-pass Bessel filter (Frequency Devices, Haverhill, MA) and digitized with a 486/33-MHz PC-compatible computer equipped with a Labmaster-TL1 data acquisition board (Axon Instruments) and pClamp 5.5 software (Axon Instruments). Cell capacitance and series resistance were maximally compensated by the circuitry of the EPC-7 amplifier. Off-line data analysis, curve fitting, and figure preparation were performed with Origin (MicroCal Software, Northampton, MA). For voltage protocols used to study I_K, leak current and capacitive artifacts were subtracted on-line by the addition of four hyperpolarizing subpulses that were one fourth of the test pulse amplitude. For peak analysis of I_A, base-line values were taken as the current at the terminal portion of each test potential ($h\infty$) in the presence of TEA-Cl (10 mM). For steady state activation/inactivation protocols, peak current (I) values were converted to conductance (G) using the equation $G = I/(E - E_K)$, where E is the test potential (in millivolts) and the reversal potential for potassium (E_K) was determined to be −80 mV. Normalized conductance values were plotted versus the test or prepulse potentials (in millivolts) for activation and inactivation protocols, respectively. The plotted values were then fit to a Boltzman function, $G/G_{max} = [1 + \exp[(V - V_{0.5})/k]]^{-1}$. Least-squares determination of the functional parameters gave values for half-activation/inactivation ($V_{0.5}$) and the slope factor (k). The I_A relative activation curve was produced similarly, with the exception that conductance values of treated cells were normalized to their paired control maximum.

A two-pulse protocol was used to determine the recovery time of I_K at −40 mV from block by 22:6n3. When equilibrium blockade with 6 μM 22:6n3 was reached, a protocol with two similar pulses was initiated, where the second test pulse was separated from the first by decreasing time intervals. Base-line was taken as the terminal part of each trace, to quantify recovery of only the blocked portion of the current. The peak current amplitude generated by each second pulse was normalized to the first and was then plotted versus the time interval between pulses. To determine τ recovery, the scatter plot of these data was fit to a monoexponential association function; values are reported in Results.

Dose-response curves were produced by plotting normalized current values and were then fit by the least-squares method using a logistic equation, percentage $I_{max} = 100/I_{max}[1 + (IC_{50}/[PUFA]n_H)]$, where I_{max} is the maximal K^+ current, IC_{50} is the concentration of 22:6n3 eliciting half-maximal inhibition, and n_H is the Hill coefficient.

The results are expressed as mean ± standard error, and p values represent the results of independent t tests (except as noted). Multiple comparisons made in Fig. 2D have taken into account the Bonferroni correction method for modified t statistics.

Results

Characteristics of cells and passive membrane properties. Electrophysiological recordings were performed on primary cultures prepared from the pineal glands of newborn rats, using whole-cell and outside-out configurations of the patch-clamp technique. Cell bodies of pinealocytes studied were roughly spherical in shape (diameter, <6 μm), with few, narrow, and short processes. The resting membrane potential was measured in 31 cells and was found to have a mean value of −51 mV ± 1.8 (range, −36 to −62 mV). Cell input resistance and capacitance (n = 20 cells) were determined, and mean values were 2.90 ± 0.28 GΩ and 0.56 ± 0.06 pF, respectively.

Characterization of voltage-activated potassium currents in pinealocytes. Pinealocytes were voltage-clamped to a holding potential of −40 mV. Depolarizing voltage steps of

increasing amplitude resulted in the activation of a family of cesium-sensitive outward currents (n = 15 cells) (data not shown) with distinct kinetics depending upon the presence (Fig. 1, A_1 and B_1) or absence (Fig. 1, A_2 and B_2) of a 400-msec conditioning prepulse to −80 mV. Depolarizing steps from −40 mV elicited a family of sustained outward currents demonstrating graded voltage-dependent activation kinetics and slowly deactivating tail currents. The threshold of activation for the current was observed at −30 mV, and half-activation was calculated to be −10 mV (k = 9) (see Fig. 4). In 15 cells, the rapid replacement of standard 1 mM $CaCl_2$ solution with nominally Ca^{2+}-free solution did not result in a decrease in current amplitude or an alteration in kinetics (data not shown). For 16 of 17 cells tested (data not shown), charybdotoxin (up to 100 nM) did not block the current. However, in one cell the application of 10 nM charybdotoxin resulted in a reversible 12% reduction in mean current amplitude with no change in current kinetics. From the results described above, the sustained outward current under our conditions is characteristic of a I_K type of potassium current.

When a preceding hyperpolarizing prepulse to −80 mV was applied, depolarizing steps often elicited I_A with rapid activation and inactivation kinetics, distinct from and superimposed upon the sustained outward current (I_K). In about 50% of pinealocytes I_A was observed; the other half expressed only I_K or had a minor component of I_A. The incidence (10 of 20 cells) was determined in three separate control groups.

TEA-Cl (10 mM) was added to external solutions to selectively attenuate I_K. TEA was effective at selectively reducing the sustained outward current for all voltage protocols; however, complete isolation by purely pharmacological means was rarely obtained (Fig. 1B). For analysis requiring fine kinetic distinctions, the residual I_K (Fig. 1, A_3 and B_3) was later digitally subtracted off-line from results from a similar protocol without the preceding hyperpolarizing prepulse.

Effects of PUFAs on I_K in pinealocytes. Pinealocytes were voltage clamped at −40 mV in the whole-cell configuration. Upon stabilization of I_K elicited by repetitive voltage steps to +60 mV (0.2–0.03 Hz), fatty acids (vehicle, 0.1% EtOH) were rapidly applied extracellularly in their dissociated free carboxyl form. In addition, PUFA was applied by bath (n = 6) (data not shown) with similar results but slower onset.

Fig. 2 demonstrates peak and kinetic modifications of I_K by 22:6n3. In general, the onset of current depression was routinely observed in the pulse immediately after drug application, steady state responses were obtained within 1 min, and the time required to reach a steady state was decreased with increasing 22:6n3 concentrations. At equilibrium, the current decay followed a monoexponential time course that approached a plateau level and was concentration dependent (Fig. 2A).

As shown in Fig. 2B, block onset proceeded rapidly and the current amplitude was recoverable within 5 min of 22:6n3 washout. In Fig. 2C, the steady state effect of 22:6n3 at different concentrations is illustrated. The minimal effective concentration of 22:6n3 affecting I_K was 1 μM, and complete blockade was observed between 25 μM and 50 μM. The IC_{50} value was 2.5 ± 0.3 μM (n = 32 cells, Hill coefficient = 1.5).

To determine the structural requirements of the fatty acid to produce this effect, we compared the effects of several fatty acids at a concentration of 6 μM (Fig. 2D). To determine the effect of chain length and unsaturation, synthetic 22-carbon fatty acids were compared with their precursor 20-carbon fatty acids with the same degree of unsaturation. The amounts of block produced by 22:4n6 and 22:5n3 were both slightly greater than but not significantly different from ($p > 0.05$) those produced by 20:4n6 and 20:5n3, respectively. In contrast, the number of double bonds significantly altered the effect of 20- and 22-carbon fatty acids. The most unsaturated fatty acid studied, 22:6n3, was the most active of all compounds tested.

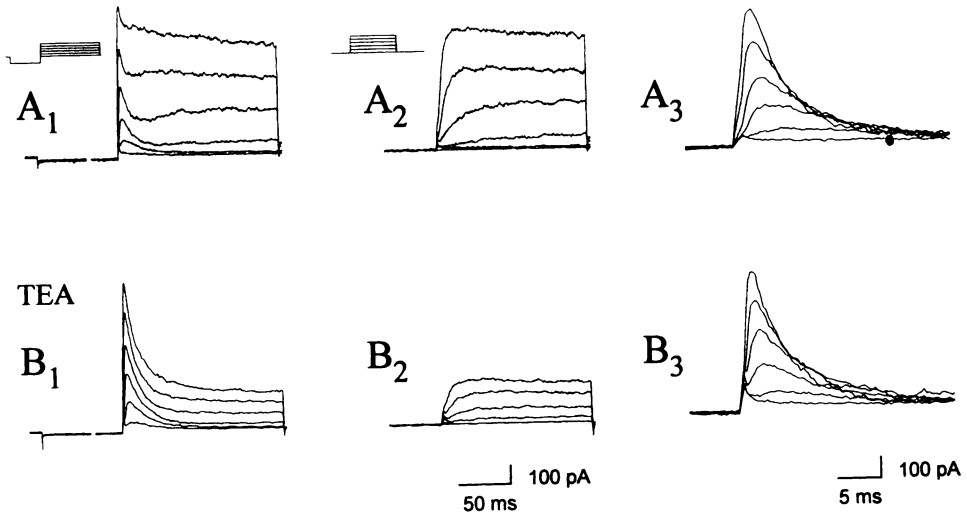

Fig. 1. Characterization of potassium currents in dissociated pinealocytes. When added to control solutions (A), TEA-Cl (10 mM) selectively attenuated I_K (B). Capacitive currents have been partially blanked, and 400-msec conditioning prepulses are displayed on a split time scale. For the pinealocytes studied, the mean cell input resistance was 2.90 ± 0.28 GΩ and cell bodies were <6 μm in diameter (traces are not leak subtracted). A_1 and B_1, Depolarizing voltage steps from the holding potential of −40 mV (maximum, +35 mV; 15-mV steps) preceded by a hyperpolarizing prepulse to −80 mV often elicited I_A (with rapid activation and inactivation kinetics), which was distinct from and superimposed upon the sustained outward current (I_K). A_2 and B_2, A similar voltage step protocol without a hyperpolarizing prepulse elicited only a family of sustained outward currents demonstrating graded voltage-dependent activation kinetics characteristic of I_K. The threshold of activation for I_K was observed at −30 mV and half-activation was calculated to be −10 mV (k = 9). *Calibration bars* apply to all traces in A_1, A_2, B_1, and B_2. A_3 and B_3, Digital subtraction of the initial segment of traces in A_1, A_2, B_1, and B_2 was used to isolate the I_A. *Calibration bars* apply to traces in A_3 and B_3.

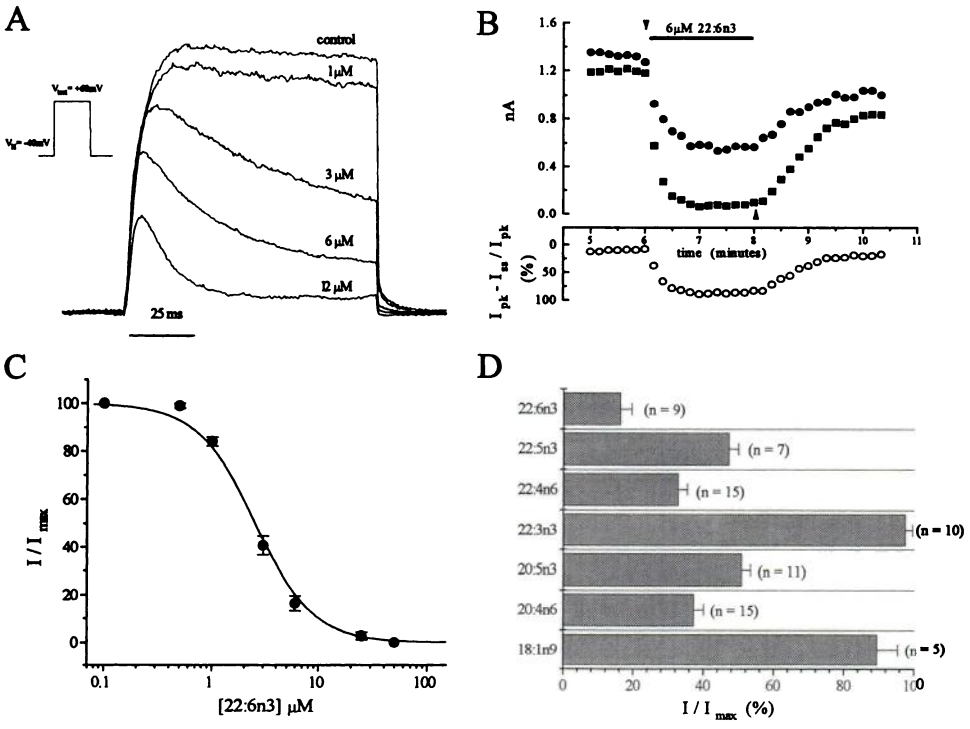

Fig. 2. Effects of PUFAs on I_K in pinealocytes. Free fatty acids (vehicle, 0.1% EtOH) were rapidly applied extracellularly while the voltage was stepped from the holding potential of −40 mV to +60 mV. A, Peak and kinetic modifications of I_K by 22:6n3. At equilibrium block, I_K follows a monoexponential decay that is concentration dependent. Tail currents were similarly reduced (normalized traces from separate experiments). B, *Upper*, time course of the 22:6n3 (6 μM) effect. The current amplitudes at the peak (●) and the end (■) of a 100-msec voltage step are plotted versus time after a 5-min period of stabilization in whole cells. *Lower*, time course and reversibility of the kinetic modifications of I_K, quantified as $[(I_{peak} - I_{plateau})/I_{peak}] \times 100$, for each trace. C, Dose-response curve for the 22:6n3 effect on I_K. The IC_{50} value for the plateau current was 2.5 ± 0.3 μM, and the Hill coefficient was 1.5 (n = 32 cells). D, Comparison of steady state block by various fatty acids (6 μM), illustrating the structural dependence on polyunsaturation.

Comparing fatty acids with four and five double bonds, both 20:4n6 and 22:4n6 had a greater effect on I_K than did 20:5n3 and 22:5n3, respectively ($p < 0.01$). Due to the unavailability of these fatty acids in both n-3 and n-6 configurations, it could not be readily determined whether the four-double bond fatty acids were more active than five-double bond compounds because of the positions of their double bonds or the degree of unsaturation. The 22-carbon fatty acid with three double bonds, 22:3n3, did not significantly ($p > 0.05$) alter I_K from control, demonstrating the importance of polyunsaturation to produce this effect. The monounsaturated fatty acid 18:1n9 was ineffective, at 6 μM, in three of the five cells tested. At concentrations up to 50 μM, 18:1n9 and 22:3n3 were only able to produce slight amplitude reduction or acceleration of the current decay, demonstrating the low efficacy of these compounds.

The resting membrane potential, input resistance, and cell capacitance were routinely recorded, and analysis revealed that they were not significantly affected by PUFAs (<50 μM) and/or the vehicle used. Later experiments with 22:6n3 did not include 0.1% EtOH as a vehicle because there was no change in the block produced by 22:6n3 with or without vehicle.

Evidence that PUFAs bind to an external site not mediated via enzymatic metabolites or protein kinase. To determine the sideness of the 22:6n3 effect, we performed a series of experiments to investigate whether the actions of 22:6n3 on I_K were observable in different membrane configurations. To outside-out macropatches (n = 12), 22:6n3 was rapidly applied while recording currents were elicited by voltage steps from −40 mV to +40 mV (data not shown). In outside-out patches, 22:6n3-induced decay of multichannel currents reached equilibrium within 10 sec after 22:6n3 application. Macropatch experiments were also performed with nominally Ca^{2+}-free extracellular solutions and intracellular solutions with no added ATP or GTP (n = 5). Under these conditons, which should deplete second messenger systems, no change in 22:6n3 block was observed.

In whole-cell experiments, internally applied 22:6n3 (12.5 μM) was ineffective at blocking or altering the kinetics of either I_A or I_K for dialysis periods of up to 10 min. These experiments were performed by either filling (n = 12) or backfilling (n = 2) patch electrodes with standard KCl solution to which 22:6n3 (0.1% EtOH) had been added. In backfilled electrodes, the tip was filled by being dipped in standard intracellular solution before the shaft of the electrode was filled with intracellular solution plus 22:6n3. In cells internally dialyzed with 22:6n3 (12.5 μM) for 10 min, the external application of 6 μM 22:6n3 promptly blocked I_K.

Inhibitor experiments were also performed to determine whether metabolic pathways, especially the lipoxygenase pathway, which is unique to the pineal gland (10), mediate the effects of 22:6n3. Inhibitors of second messenger and fatty acid metabolic pathways were determined to have no effect on the action of 22:6n3 on I_K. Protein kinase inhibitors H-7 (100 nM) (n = 7) or staurosporine (100 μM) (n = 5), dialyzed internally for periods of up to 10 min, had no effect on the reponse to 6 μM 22:6n3. In nominally calcium-free medium, 22:6n3 reduced I_K by 80% (n = 4), which was not different from the value reported in standard 1 mM calcium solutions. P450 enzymes metabolize various fatty acids; however, the P450 inhibitors metyrapone (50 μM) and SKF-525A (Proadifen-HCl, 50 μM) also failed to inhibit the effect of 22:6n3 (n = 7). ETYA (12 μM), a pseudosubstrate inhibitor of cyclooxygenase/lipoxygenase pathways as well as P450 enzymes, was included in the patch electrode (n = 4). Intracellular ETYA did not inhibit the effect of 6 μM 22:6n3. However, extracellularly applied ETYA produced a direct block of I_K and accelerated current decay, similarly to other PUFAs. Although it was less potent than 22:6n3, the application of 25 μM ETYA resulted in a 79% reduction in mean I_K.

I_A in pinealocytes is blocked by PUFAs. To investigate the effect of PUFA on I_A and to rule out possible interference

with our measurements of I_K, fatty acids were rapidly applied to cells voltage-clamped at −40 mV in the presence of 10 mM TEA-Cl. K^+ currents were activated by depolarizing incremental voltage steps to +35 mV, each being preceded by a 400-msec conditioning prepulse to −80 mV. From a logistic curve fit of the peak I_A dose-response curve for 22:6n3 (n = 20 cells), we estimated the half-maximal inhibitory dose to be 2.0 ± 0.1 μM at +35 mV. Increasing concentrations of 22:6n3 resulted in combined peak reduction and acceleration of macroscopic inactivation qualitatively similar to that described for I_K. We believe that the steepness of the dose-response relationship (Hill coefficient of 3.0) may reflect an increasing overlap with capacitive current; therefore, our assessment of the IC_{50} may be a slight underestimate. Similar results were obtained in the absence of TEA-Cl, demonstrating the simultaneous action of increasing doses of 22:6n3 on both I_A and I_K (Fig. 3B, *inset*). The macroscopic inactivation rate of the I_A was fit with a biexponential function, and in Table 1 are summarized the time constants (τ) for the fast component of inactivation (n = 6 cells).

We then investigated the voltage-dependent effects of fatty acids on the I_A at 1 μM (6–9 cells/group). Conductance-voltage curves were constructed as described in Materials and Methods. Values were plotted and then fit to a Boltzman function, $G/G_{max} = [1 + \exp[(V - V_{0.5})/k]]^{-1}$ (Fig. 3C). In control solutions, best-fit parameters for half-inactivation and half-activation were −68.9 mV (k = 6.44) and +7.03 mV (k = 19), respectively. PUFAs did not significantly affect the steady state activation curve, whereas a hyperpolarizing shift was seen for steady state inactivation. Specifically, 20:5n3 and to a lesser extent 20:4n6 (data not shown) were able to shift the midpoint of inactivation by −7 mV ($p < 0.01$) and −3 mV, respectively. This resulted mainly from a change in the slope of the Boltzman function (k) from 6.5 ± 0.5 (control) to 4.5 ± 0.5 (20:5n3).

Voltage dependence of 22:6n3-induced block of I_K. To further investigate the possible mechanism of 22:6n3-induced changes in current kinetics, the current-voltage relationship was examined (Fig. 4). The percentage block of I_K, measured at steady state, by 3 and 6 μM 22:6n3 increased with voltage and then remained relatively constant. The small but significant increase in block for more negative potentials corresponds to the voltage region where the channels are most likely to undergo the gating transition from closed to open (see Fig. 4A, *inset*). Beyond the gating region, the percentage of block measured at steady state was not significantly affected by voltage ($p > 0.05$). The steady state activation curve (see Fig. 4A, *inset*) was constructed by measuring peak tail currents (−35 mV) at the end of test steps used for experiments in Fig. 4A. The leftward shift in the half-activation value from −10 mV to −23 mV (3 μM 22:6n3) corresponds to the voltage dependence of 22:6n3 block. That is, the peak tail current reaches a maximum at more negative potentials because fractional I_K block increases at potentials in the gating region. Moreover, the measured threshold for activation was unchanged at about −30 mV and fractional block was at its minimum.

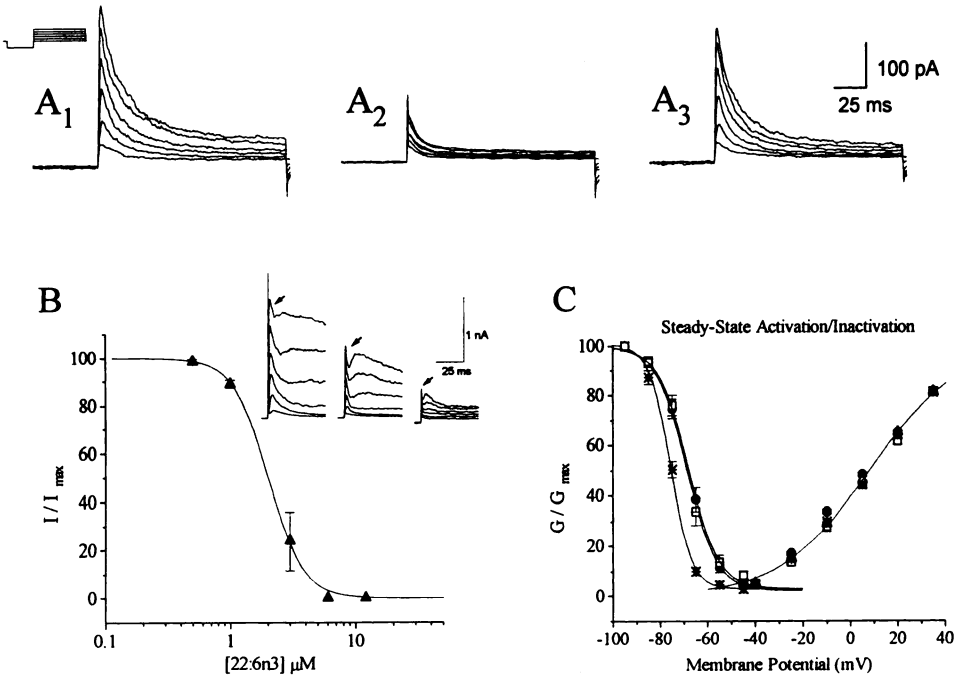

Fig. 3. Block of I_A in pinealocytes by PUFAs. Fatty acids were applied to pinealocytes voltage-clamped at −40 mV, in the presence of 10 mM TEA-Cl to selectively block I_K. A, Currents activated by depolarizing incremental voltage steps (maximum, +35 mV; 15 mV steps), each preceded by a 400-msec conditioning prepulse to −80 mV. A_1, These steps elicited currents with rapid activation and inactivation kinetics, distinct from the residual I_K. A_2, 22:6n3 (6 μM) effectively decreased I_A for all test potentials. A_3, Upon wash-out of 22:6n3 and exchange with the vehicle (0.1% EtOH), recovery was obtained (~3 min). B, Concentration-effect relationship between 22:6n3 and I_A. The half-maximal inhibitory dose (IC_{50}) of peak I_A was 2.0 ± 0.1 μM. *Inset*, as increasing doses of 22:6n3 (*left*, control; *middle*, 3 μM; *right*, 12 μM 22:6n3) are applied, peak I_A overlaps with the capacitive current; the traces illustrate the effect of 22:6n3 in the absence of TEA-Cl, demonstrating the simultaneous actions on I_A (*arrows*) and I_K. C, Effect of various fatty acids (1 μM) on the voltage dependence of I_A (n = 6–9 cells/group). Peak conductance, expressed as percentage, is plotted versus the test potential for steady state activation or the prepulse potential for steady state inactivation. From a fit of the data to the Boltzman equation, it was determined that PUFAs did not affect the steady state activation curve ($h_{0.5}$ = −7.03 mV, k = 19). The steady state inactivation curve ($h_{0.5}$ = −68.9 mV, k = 6.44) was shifted by 20:5n3 to the left by −7 mV and the slope factor (k) was decreased to 4.5; 22:6n3 and 20:4n6 ($h_{0.5}$ = −72 mV) (not shown) did not significantly shift the curve at this concentration (●, control; □, 22:6n3; *, 20:5n3; △, 20:4n6).

TABLE 1

Macroscopic inactivation rate of I_A is increased by 1 μM 22:6n3

Decay time constants (τ_{fast}) represent the mean ± standard error of values for the fast component of a biexponential decay function; the slow component comprises only a small fraction of the total current and is not represented here. Levels of significance were determined by paired *t* tests for $n = 6$ pinealocytes

Test potential	τ_{fast}	
	Control	1 μM 22:6n3
mV	*msec*	
+35	9.33 ± 0.67	5.25 ± 0.27[a]
+20	10.2 ± 0.3	6.01 ± 0.35[b]
+5	14.6 ± 0.7	7.58 ± 0.62[a]
−10	14.1 ± 1.2	8.99 ± 1.18[b]

[a] $p < 0.0005$.
[b] $p < 0.005$.

Some pinealocytes also possessed a slowly developing (~100-msec) inward current activated by hyperpolarizing voltage steps, as previously noted by others (12). Voltage- and current-clamp analyses of this inward rectifier show that it resembles the current known as I_H (21, 22). Characteristic of I_H, the inward current was noninactivating, had slow activating/deactivating kinetics, and was completely blocked by external cesium (5 mM, $n = 4$ cells) (data not shown). The inwardly rectifying portion of the current-voltage curve was unaffected by 22:6n3 (Fig. 4C). For the purposes of our K^+ current studies, pinealocytes with I_H were excluded from I_A experimental groups because the deactivation of I_H could prevent the accurate measurement of I_A.

Kinetic analysis of the time dependence of 22:6n3-induced block. The transition in the shape of current traces from noninactivating to inactivating with externally applied 22:6n3 can be explained by an accumulation of block during the time course of each depolarizing voltage step. To quantify the time course of voltage-dependent drug binding and unbinding rates, the decay rate of I_K was examined for different voltages and concentrations of 22:6n3. Percentage block values were calculated for each data point of the current record acquired during 200-msec (6 μM, $n = 3$) or 300-msec (3 μM, $n = 4$) test steps to potentials between +8 and +40 mV. As illustrated in Fig. 5A, the percentage of block increases along a monoexponential time course that can be fitted to the equation

$$A_t = A_0 \exp(-t/\tau) + A_1[1 - \exp(-t/\tau)] \quad (1)$$

where A_t is the percentage block at time t and A_0 and A_1 are the percentage block values at the beginning and end of the voltage step, respectively. The time constant (τ) is the time required for block to reach 50% of its equilbrium value. The test step duration was at least 4 times the average τ value, to best approximate the approach to equilibrium block for a given concentration of 22:6n3. For the example illustrated, block increased from an initial value of 5.7% to 90% along a time course of $\tau = 16$ msec.

Based on the concentration-effect curve (Fig. 2C) and assuming first-order kinetics for a simple one-to-one binding reaction between 22:6n3 and the K^+ channel, the rate constant $k_{app} = 1/\tau$ for approach to equilibrium is related to the binding (k_1) and unbinding (k_{-1}) rates by

$$k_{app} = k_1[22{:}6n3] + k_{-1} \quad (2)$$

Substituting K_d for k_1 and k_{-1}, because $K_d = k_{-1}/k_1$, we obtain eqs. 3 and 4.

$$k_1 = k_{app}/([22{:}6n3] + K_d) \quad (3)$$

$$k_{-1} = k_{app}/([22{:}6n3]/K_d + 1) \quad (4)$$

The values plotted in Fig. 5B were calculated from eqs. 3 and 4 by using $IC_{50} = 2.6$ μM as the apparent K_d, with values of k_{app} determined by fitting the data to eq. 1. To obtain roughly similar values for on- and off-rate constants, k_1 and k_{-1}, τ had to decrease as the 22:6n3 concentration was increased. Similarly to the steady state blocking effect reported in Fig. 4B, the on- and off-rate constants were relatively independent of voltage. The slight decreases in plotted rate constants at more positive

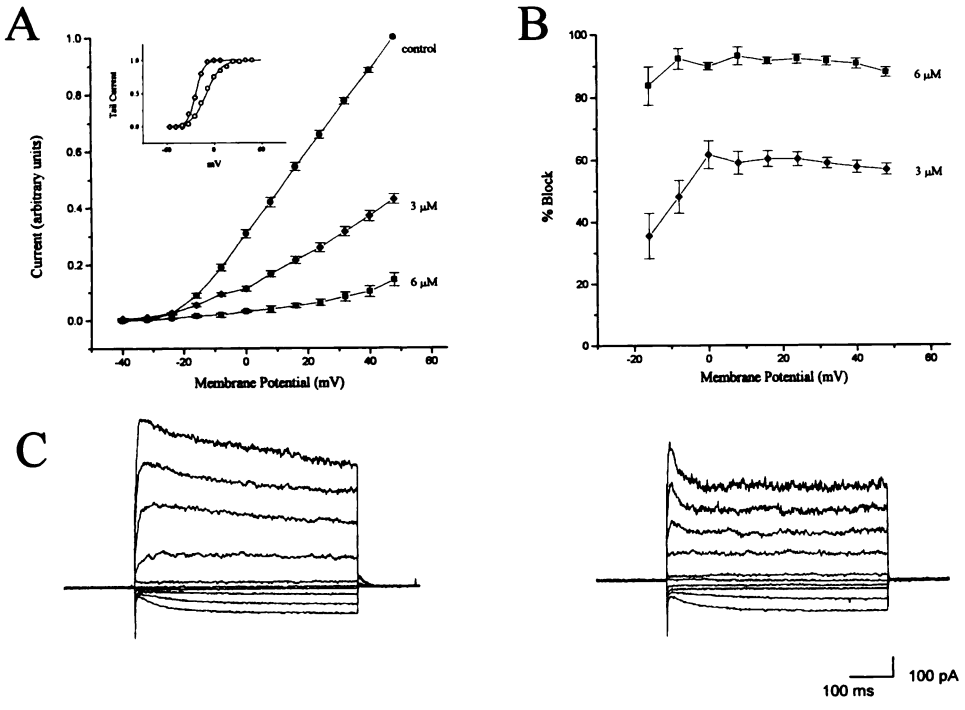

Fig. 4. Voltage dependence of 22:6n3 block of I_K. A, Voltage dependence of 22:6n3 block. The effect of 3 μM (♦) and 6 μM (■) 22:6n3 on the leak-subtracted current-voltage relationship was compared with control values (●) measured at the terminal portion of increasing voltage steps (holding potential, −60 mV). *Inset*, the leftward shift (−13 mV) in the steady state activation curve (normalized peak tail currents) illustrates increasing fractional blockade at potentials in the I_K activation region (◇, 3 μM 22:6n3; ○, control). B, Fractional blockade (percentage) of the I_K calculated from current values in A. C, *Left*, example of the current-voltage relationship in a pinealocyte (control). *Right*, block of outward but not inward rectification by 22:6n3 (3 μM). Currents were evoked by 500-msec voltage steps to varying potentials (minimum, −120 mV; maximum, +80 mV).

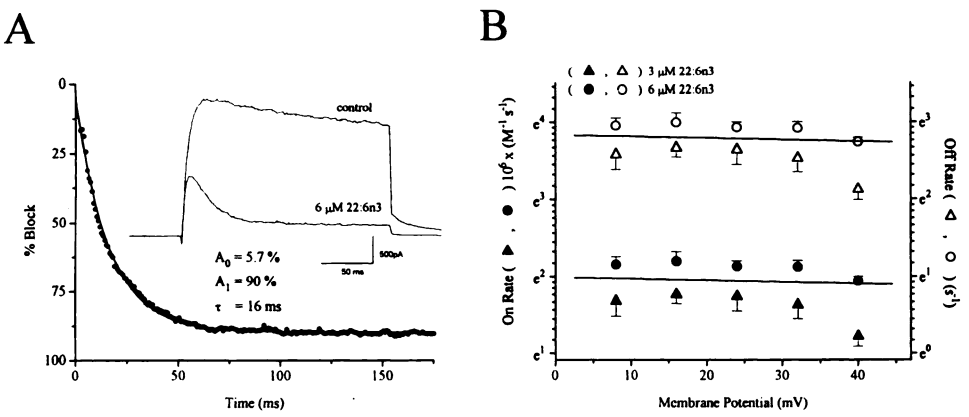

Fig. 5. Time dependence of 22:6n3 block of I_K. A, To quantify the time course of drug association with the K^+ channel, percentage block values were calculated for each data point of the current record acquired during voltage steps to potentials between +8 and +40 mV. In the example shown, blockade of the current increases along a monoexponential time course with initial amplitude of $A_0 = 5.7\%$ to a steady state value of $A_1 = 90\%$ with a time constant (τ) of 16 msec. B, The rates of 22:6n3 binding and unbinding during voltage steps were determined. On-rate (k_1) and off-rate (k_{-1}) constants were calculated as described in the text ($n = 7$ cells).

potentials were not statistically significant and would not explain time-dependent changes in I_K produced by 22:6n3.

For the percentage block to follow the time course illustrated, a large fraction of channels must become unblocked upon repolarization. To determine the dissociation time constant of 6 μM 22:n3 at the holding potential, recovery from block was estimated with a two-pulse protocol (see Materials and Methods) once steady state block was reached. The time required to relieve 50% of steady state block was estimated to be 230 ± 28 msec ($n = 4$ cells).

In the presence of 5 mM 4-AP, the current decay induced by 22:6n3 was not as apparent. In addition, 4-AP significantly ($n = 12$ cells, $p < 0.001$) slowed the activation kinetics (τ_{rise}) of the I_K for all potentials studied (Fig. 6C). This effect on the shape of I_K can be predicted based on voltage-dependent unbinding of 4-AP from its site during the depolarizing test step (23, 24). The steady state concentration-effect curves for 22:6n3 in the presence ($n = 14$ cells) and absence ($n = 32$ cells) of 4-AP are shown in Fig. 6B. The IC_{50} values were not significantly affected by 4-AP (control, 2.5 ± 0.3 μM; 4-AP, 2.8 ± 0.4 μM). For the experiment illustrated (Fig. 6A), a point-by-point analysis of the approach to steady state block revealed that the k_{app} values are equal and that reaction kinetics with 22:6n3 are unchanged. Therefore, although the shape of current traces are visibly altered, it appears that 22:6n3 and 4-AP act independently of each other.

Group IIb metal antagonism of 22:6n3 block of I_A and I_K. 22:6n3 was rapidly applied in the presence of zinc (or cadmium) and found to efficaciously inhibit PUFA blockade of both I_A and I_K ($n = 17$ cells). When zinc (100 μM) was applied, the well reported depolarizing "shifts" of the steady state inactivation and activation of I_A (25–27) occurred as rapidly as the solutions could be exchanged. Increasing the zinc concentration from 100 μM to 1 mM only slightly enhanced the depolarizing shift. Application of 12 μM 22:6n3 in the presence of 1 mM zinc resulted in a minimal current reduction (Fig. 7A). Block by 22:6n3 and/or "unshifting" of I_A was promptly observed when zinc was washed out. Conversely, 12 μM 22:6n3 added in the presence of 100 μM zinc resulted in a significant amount of block, which was surmountable by increasing the zinc concentration to 1 mM (Fig. 7B). Fig. 7C illustrates a similar experiment with I_K in a cell possessing a relatively small

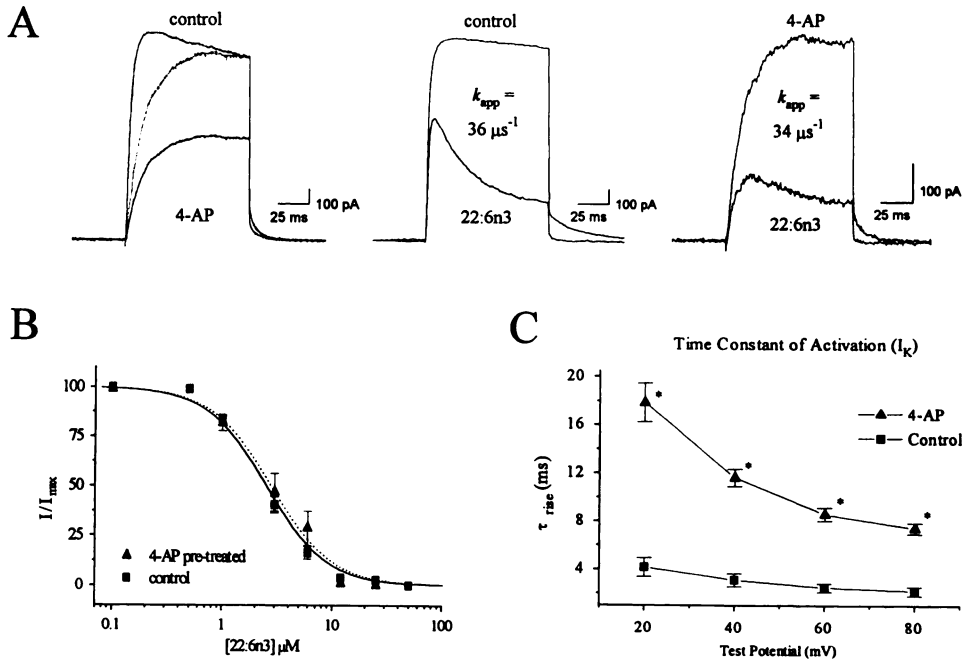

Fig. 6. Lack of effect of 4-AP on the time course of 22:6n3 block. A, 4-AP blocked the I_K and changed the shape of the current (holding potential, −40 mV) (*left*). *Dotted line*, 4-AP trace scaled to control amplitude. In the presence of 5 mM 4-AP (*right*), the acceleration of current decay induced by 22:6n3 (6 μM) was not as apparent, compared with control (*middle*), whereas the time course of block (k_{app}) was unaffected. B, The dose-response relationship between 22:6n3 and I_K was not affected by pretreatment with 4-AP (control, $IC_{50} = 2.5 \pm 0.3$ μM; 4-AP, $IC_{50} = 2.8 \pm 0.4$ μM). C, The time constant of activation (τ_{rise}) was significantly increased by 5 mM 4-AP at all test potentials ($n = 12$ cells). *, $p < 0.001$.

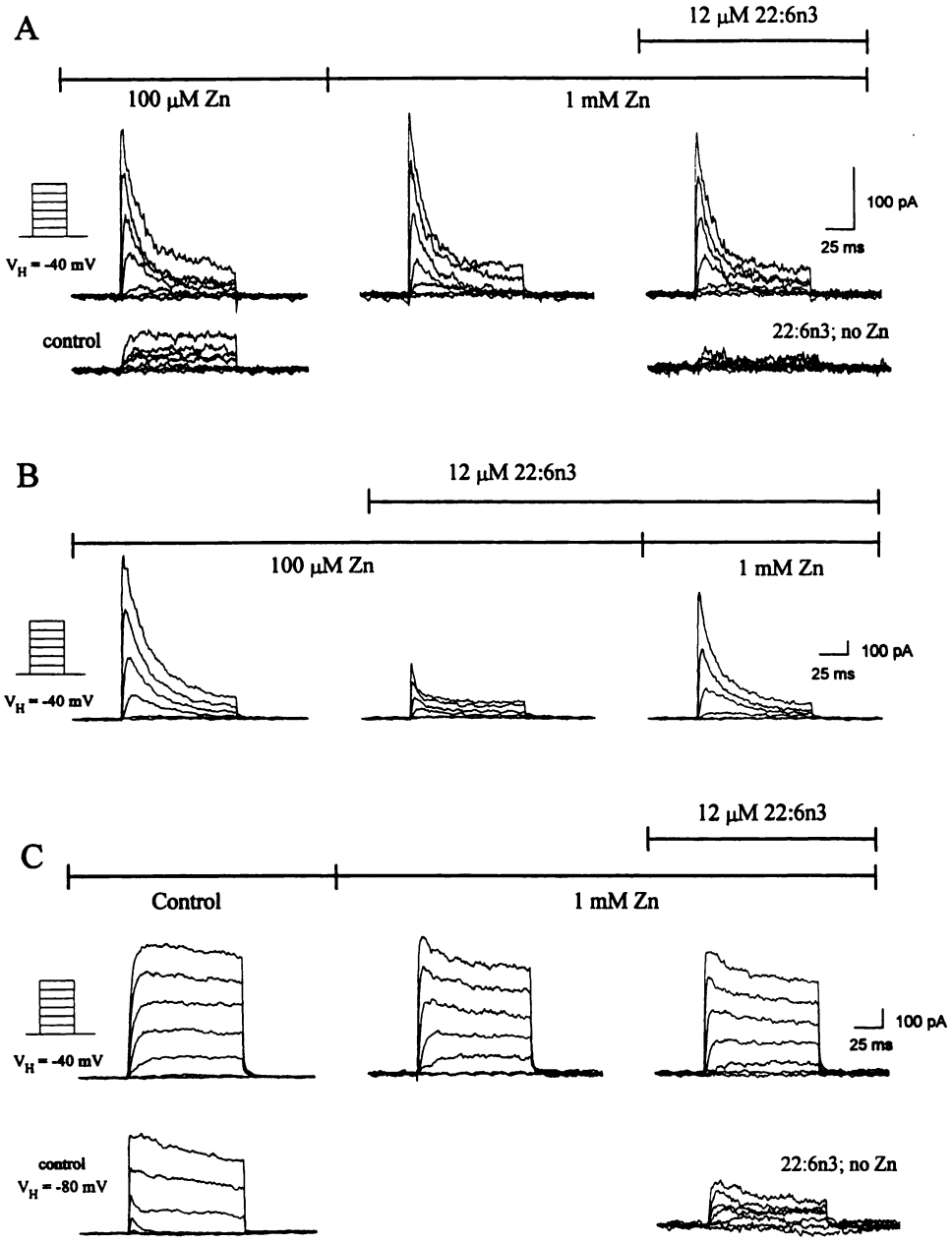

Fig. 7. Zinc inhibition of 22:6n3 blockade of K^+ currents. Zinc antagonized the 22:6n3-induced blockade of I_A and I_K. *Bars*, exchange of external solutions containing zinc and/or 22:6n3, as indicated. A, Rapid application of zinc (100 μM) resulted in a large inactivating current being elicited, due to the summation of shifted I_A and unshifted I_K. Coapplication of 22:6n3 (12 μM) with 1 mM zinc resulted in a minimal reduction of current. Reduction and/or unshifting was observed upon zinc wash-out (*lower right*). B, In a similar experiment, 22:6n3 (12 μM) was applied in the presence of 100 μM zinc. In contrast to A, 100 μM zinc only partially antagonized 22:6n3 effects, and the antagonism was partially surmountable by the coapplication of 1 mM zinc. C, In a pinealocyte expressing mainly I_K, 22:6n3-induced blockade of I_K was similarly prevented by 1 mM zinc. Block was promptly observed upon zinc wash-out (*lower right*).

I_A. Similarly to zinc, cadmium also caused the depolarizing shift of I_A and antagonized 22:6n3 block (n = 9 cells).

Discussion

PUFA modulates potassium currents in pinealocytes. Membrane currents recorded from dissociated cells of the rat pineal gland have been characterized by the patch-clamp technique. Based on pharmacological and kinetic analyses of outward current, the pinealocytes possess at least two distinct voltage-gated K^+ currents, 1) a sustained outward current (I_K) and 2) an I_A. The proportions of these two current types were variable from cell to cell, and only about 50% of pinealocytes possessed I_A.

The ω-3 fatty acid 22:6n3 not only depressed peak current but also produced a striking decay of I_K. To determine the structural requirement of the fatty acid to produce this effect on I_K, we compared the effects of several fatty acids. The 20-carbon fatty acids 20:5n3 and 20:4n6 were compared with 22-carbon elongation products (22:5n3 and 22:4n6). Although these PUFAs have different chain lengths, block produced by the 22-carbon compounds was not different from that produced by their 20-carbon precursors. In contrast, the number of double bonds significantly altered the effects of 20- and 22-carbon fatty acids. Interestingly, a simple graded response did not occur when different fatty acids of increasing unsaturation were tested. For example, the 22-carbon fatty acid with three double bonds was almost inactive, whereas 22:4n6 blocked I_K by 63% (6 μM). This result suggests that the minimum requirement to obtain a high degree of activity is four double bonds. Molecular dynamic simulations have suggested that PUFAs such as 20:4n6 can preferentially interact with proteins based on their ability to assume tightly packed conformations (28).

Kinetic changes in outward current are not due to a PUFA-resistant I_A. The steady state inactivation curve for

I_A indicates that at a holding potential of −40 mV I_A is nearly 100% inactivated. The unmasking of a resistant I_A by a selective blocker of I_K would require the simultaneous depolarizing shift of steady state inactivation. On the contrary, doses of PUFA that do not completely block I_A have been demonstrated to shift the steady state inactivation in the hyperpolarizing direction (Fig. 3C). Moreover, the I_A was more potently blocked by 22:6n3 than was the I_K. Experiments performed on the combined I_A and I_K (Fig. 3B, *inset*) failed to demonstrate a decrease in the sensitivity of I_A to 22:6n3 in the absence of TEA-Cl. These results confirm that the kinetic modulation of I_K is not due to a resistant I_A.

Direct ion channel interaction or second messenger-mediated effect? Fatty acids have been demonstrated to directly interact with ion channels (14, 29). However, the possibility that the action of 22:6n3 and related fatty acids may be mediated through oxygenated metabolites or second messenger systems must be addressed. Unlike 20:4n6, 22:6n3 and 18:1n9 are not substrates for cyclooxygenase, but these fatty acids can both be metabolized in the pineal gland (10) by lipoxygenase enzymes to form stable hydroxy metabolites. Preliminary experiments indicate that the 12-lipoxygenase metabolite 14-OH-22:6n3 is less potent, with respect to the ability to block I_K, than is its precursor 22:6n3.[1] The role that lipoxygenase metabolism plays in the pineal gland remains unknown.

The second messenger hypothesis is further weakened by the finding that the protein kinase inhibitors H-7 and staurosporine did not alter the effect of 22:6n3, nor did the removal of calcium from extracellular solutions. Inhibitors of P450 enzymes also had no effect on the action of 22:6n3. The combined eicosanoid inhibitor ETYA also failed to prevent 22:6n3-induced block when dialyzed internally. Moreover, as a fatty acid analog, ETYA itself directly blocked I_K when extracelluarly applied and accelerated the current decay, similarly to other PUFAs. Internally applied 22:6n3 had no effect, suggesting that, despite the fact that PUFAs are hydrophobic compounds, as charged species they do not freely permeate biological membranes. Results with inhibitors and ETYA indicate that block is due to a direct effect at a site located on the external domain of the channel.

Voltage-dependent block is probably due to a preference for open channels. Externally applied PUFAs modified I_K in a manner similar to that described for internally applied hydrophobic TEA analogs in voltage-clamped squid giant axon and frog node of Ranvier (30–32). The pharmacological mechanism proposed for PUFAs is similar to that described for TEA analogs, such that PUFAs preferentially block the open-state channel and a large fraction of channels become unblocked in the closed state. This statement is supported by the findings that fractional blockade increased monoexponentially during the time course of each depolarizing voltage step, was concentration dependent, and was voltage independent at potentials positive to the gating region. Kinetic analysis of the time course of block by 22:6n3 was consistent with a first-order reaction. For the reaction with 22:6n3, the apparent affinity (K_d) was 2.5 μM and the rate constants k_1 and k_{-1} were approximately described by values of 6.8×10^6 M^{-1} sec^{-1} and 16 sec^{-1}, respectively. The time dependence of block was inconsistent with the possibility that 22:6n3 binds allosterically to K^+ channels, because a biexponential time course was not observed.

4-AP decreases the activation rate of I_K in pinealocytes (Fig. 4B). This result could be predicted, based on studies showing that 4-AP exhibits greater blocking ability at more negative voltages and that block is partially removed during a depolarizing test step, in a time-dependent manner (23, 24). The resulting effect would be a decrease in the current amplitude measured during the rising phase of the I_K. In the presence of 5 mM 4-AP, the current decay induced by 22:6n3 was not as apparent, despite a similar concentration-effect relationship. Therefore, although the shapes of current traces are visibly altered, 22:6n3 and 4-AP appear to act independently of each other. This is also supported by the finding that, although a significant fraction of I_K is blocked by 4-AP, a similar point-by-point time course (k_{app}) of percentage block was calculated. These results further support the hypothesis that 22:6n3 block is dependent on the channel reaching the conducting or open state.

Group IIb metals antagonize PUFA blockade of I_A and I_K. Others previously reported that group IIb metals cause a depolarizing shift in the steady state activation/inactivation ranges of I_A but not I_K (25–27). In addition to this effect, we report that both group IIb metals tested, zinc and cadmium, antagonize 22:6n3 block. Inhibition is observed not only for the shifted I_A but also for the unshifted I_K. This action of zinc may result from an allosteric mechanism that does not allow 22:6n3 access to its binding site.

Cadmium has been effectively used as a pharmacological tool to block voltage-gated calcium channels. Fortuitously, this is how we discovered that group IIb metals antagonize the block of voltage-gated K^+ channels by fatty acids. This effect was found to be independent of the presence of external calcium. We believe that this finding may explain the discrepancy found in previous reports regarding fatty acid effects on voltage-gated K^+ channels. In one study on cultured rat cortical neurons (17), 200 μM cadmium was used in all external solutions to block voltage-gated calcium channels; the results of this study reported a slight enhancement of the combined sustained and transient K^+ currents by 50 μM 20:4n6. Conversely, we have observed in cultured rat cortical neurons[2] kinetic modifications and dose-dependent blocking of K^+ currents by fatty acids, including 20:4n6, similar to those we have described in pinealocytes.

The finding that fatty acids alter the kinetics of voltage-gated K^+ currents has been reported for neuroblastoma cells (33), smooth muscle cells (34), and CA1 pyramidal neurons of the hippocampus (35). However, none of those investigators proposed a pharmacological model for the observed changes. In one recent study, however, Honoré *et al.* (16) came to the similar conclusion that the major cardiac delayed rectifier (Kv1.5) is blocked externally by PUFAs by an open-channel blocking mechansim, and certain antiarrhythmic drugs are well known to act via this mechanism. Animal studies (36, 37) have demonstrated that diets high in PUFAs but not monounsaturated fatty acids can decrease the incidence of fatal postischemic cardiac arrhythmias. These data correlate well with our finding that blockade of these K^+ channels requires a certain degree of polyunsaturation.

[1] J. S. Poling and J. W. Karanian, unpublished observations.

[2] J. S. Poling, S. Vicini, and N. Salem Jr., unpublished observations.

In brief, long-chain PUFAs blocked inactivating and noninactivating K^+ currents in pinealocytes. The blockade of I_K by PUFAs is not restricted to pinealocytes but also applies to neocortical neurons and Kv1.2 channels expressed in fibroblasts.[3] In pinealocytes, only the outwardly rectifying portion of the current-voltage curve was blocked, whereas the inward rectifier, characterized as I_H, remained insensitive to 22:6n3. Blockade of I_K by 22:6n3 was relatively voltage independent, except in the gating region of the channel. Analysis of reaction kinetics at this external binding site revealed that the rate at which block approaches equilibrium was concentration dependent and voltage independent. Our results on the time- and voltage-dependent properties of 22:6n3 block support an open-channel blocking mechanism.

Acknowledgments

We thank Dr. Michael A. Rogawski for critical reading of the manuscript and helpful comments on the kinetic analysis of our data. We would also like to thank Dr. Erminio Costa and members of the Fidia-Georgetown Institutes for the Neurosciences for their support and helpful discussions in the preparation of this manuscript.

References

1. Bang, H. O., and J. Dyerberg. Lipid metabolism and ischemic heart disease in Greenland Eskimos. *Adv. Nutr. Res.* **3**:1–22 (1980).
2. Salem, N., Jr., and G. R. Ward. Are *omega*-3 fatty acids essential nutrients for mammals? *World Rev. Nutr. Diet.* **72**:128–147 (1993).
3. Salem, N., Jr. *Omega*-3 fatty acids: molecular and biochemical aspects, in *New Protective Roles of Selective Nutrients in Human Nutrition* (G. Spiller and J. Scala, eds.). Alan R. Liss, New York, 109–228 (1989).
4. Salem, N., Jr., and C. D. Niebylski. The nervous system has an absolute molecular species requirement for proper function. *Mol. Membr. Biol.*, in press.
5. Marshall, B. H. Lipids and neurological diseases. *Med. Hypotheses* **34**:272–274 (1991).
6. Bazan, N. G., M. G. Murphy, and G. Toffano. Neurobiology of essential fatty acids. *Adv. Exp. Med. Biol.* **318**:285–306 (1992).
7. Pawlosky, R. J., A. Barnes, and N. Salem, Jr. Essential fatty acid metabolism in the feline: the relationship between liver and brain production of long chain polyunsaturated fatty acids. *J. Lipid Res.* **35**:2032–2040 (1994).
8. Hoffman, D. R., E. E. Birch, D. G. Birch, and R. D. Uauy. Effects of supplementation with *omega*-3 long-chain polyunsaturated fatty acids on retinal and cortical development in premature infants. *Am. J. Clin. Nutr.* **57**:807S–812S (1993).
9. Bazan, N. G., E. B. Rodrigues deTurco, and W. C. Gordon. Pathways for the uptake and conservation of docosahexaenoic acid in photoreceptors and synapses: biochemical and autoradiographic studies. *Can. J. Physiol.* **71**:690–698 (1993).
10. Sawazaki, S., N. Salem, Jr., and H. Y. Kim. Lipoxygenation of docosahexaenoic acid by the rat pineal body. *J. Neurochem.* **62**:2437–2447 (1994).
11. Aguayo, L. G., and F. F. Weight. Characterization of membrane currents in dissociated adult rat pineal cells. *J. Physiol. (Lond.)* **405**:397–419 (1988).
12. Freschi, J. E., and A. G. Parfitt. Intracellular recordings from pineal cells in tissue culture: membrane properties and response to norepinephrine. *Brain Res.* **368**:366–370 (1986).
13. Piomelli, D., and P. Greengard. Lipoxygenase metabolites of arachidonic acid in neuronal transmembrane signalling. *Trends Pharmacol. Sci.* **11**:367–372 (1990).
14. Ordway, R. W., J. J. Singer, and J. V. Walsh, Jr. Direct regulation of ion channels by fatty acids. *Trends Neurosci.* **14**:96–100 (1991).
15. Pepe, S., K. Bogdanov, H. Hallaq, H. Spurgeon, A. Leaf, and E. Lakatta. ω3 polyunsaturated fatty acid modulates dihydropyridine effects on L-type Ca^{2+} channels, cytosolic Ca^{2+}, and contraction in adult rat cardiac myocytes. *Proc. Natl. Acad. Sci. USA* **91**:8832–8836 (1994).
16. Honoré, E., J. Barhanin, B. Attali, F. Lesage, and M. Lazdunski. External blockade of the major cardiac delayed-rectifier K^+ channel (Kv1.5) by polyunsaturated fatty acids. *Proc. Natl. Acad. Sci. USA* **91**:1937–1944 (1994).
17. Zona, C., E. Palma, L. Pellerin, and M. Avoli. Arachidonic acid augments potassium currents in rat neocortical neurons. *NeuroReport* **4**:359–362 (1993).
18. Alho, H., C. Ferrarese, S. Vicini, and F. M. Vaccarino. Subset of GABAergic neurons in dissociated cell cultures of neonatal rat cerebral cortex show co-localization with specific modulator peptides. *Dev. Brain Res.* **39**:193–204 (1988).
19. Hamill, O. P., A. Marty, E. Neher, B. Sakmann, and F. J. Sigworth. Improved patch-clamp technique for high-resolution current recording from cells and cell-free membrane patches. *Pflügers Arch.* **391**:85–91 (1981).
20. Murase, K., P. D. Ryu, and M. Randic. Excitatory and inhibitory amino acids and peptide-induced responses in acutely isolated rat spinal dorsal horn neurons. *Neurosci. Lett.* **103**:56–63 (1989).
21. DiFrancesco, D. A study of the ionic nature of the pace-maker current in calf Purkinje fibres. *J. Physiol. (Lond.)* **314**:377–393 (1981).
22. Schlichter, R., C. R. Bader, and L. Bernheim. Development of anomolous rectification (I_H) and of a tetrodotoxin-resistant sodium current in embryonic quail neurones. *J. Physiol. (Lond.)* **442**:127–145 (1990).
23. Kirsch, G. E., and J. A. Drewe. Gating-dependent mechanism of 4-aminopyridine block in two related potassium channels. *J. Gen. Physiol.* **102**:797–816 (1993).
24. Choquet, D., and H. Korn. Mechanism of 4-aminopyridine action on voltage-gated potassium channels in lymphocytes. *J. Gen. Physiol.* **99**:217–240 (1992).
25. Mayer, M. L., and K. Sugiyama. A modulatory action of divalent cations on transient outward current in cultured rat sensory neurones. *J. Physiol. (Lond.)* **396**:417–433 (1988).
26. Agus, Z. S., I. D. Dukes, and M. Morad. Divalent cations modulate the transient outward current in rat ventricular myocytes. *Am. J. Physiol.* **261**:C310–C318 (1991).
27. Harrison, N. L., H. K. Radke, G. Talukder, and J. M. H. ffrench-Mullen. Zinc modulates transient outward current gating in hippocampal neurons. *Recept. Channels* **1**:153–163 (1993).
28. Rich, M. R. Conformational analysis of arachidonic acid and related fatty acids using molecular dynamic simulations. *Biochim. Biophys. Acta* **1178**:87–96 (1993).
29. Ordway, R. W., J. V. Walsh, Jr., and J. J. Singer. Arachidonic acid and other fatty acids directly activate potassium channels in smooth muscle cells. *Science (Washington D. C.)* **244**:1176–1179 (1989).
30. Armstrong, C. M. Interaction of tetraethylammonium ion derivatives with the potassium channels of giant axons. *J. Gen. Physiol.* **58**:413–437 (1971).
31. French, R. J., and J. J. Shoukimas. Blockage of squid axon potassium conductance by internal tetra-*N*-alkylammonium ions of various sizes. *Biophys. J.* **34**:271–291 (1981).
32. Armstrong, C. M., and B. Hille. The inner quaternary ammonium ion receptor in potassium channels of the node of Ranvier. *J. Gen. Physiol.* **59**:388–400 (1972).
33. Rouzaire-Dubois, B., V. Gérard, and J. M. Dubois. Modification of K^+ channel properties induced by fatty acids in neuroblastoma cells. *Pflügers Arch.* **419**:467–471 (1991).
34. Shimada, T., and A. P. Somlyo. Modulation of voltage-dependent Ca current by arachidonic acid and other long-chain fatty acids in rabbit intestinal smooth muscle. *J. Gen. Physiol.* **100**:27–44 (1992).
35. Keyser, D. O., and B. E. Alger. Arachidonic acid modulates hippocampal calcium current via protein kinase C and oxygen radicals. *Neuron* **5**:545–553 (1990).
36. McLennan, P. L. Relative effects of dietary saturated, monounsaturated, and polyunsaturated fatty acids on cardiac arrhythmias in rats. *Am. J. Clin. Nutr.* **57**:207–212 (1993).
37. McLennan, P. L., L. R. Barnden, T. M. Bridle, M. Y. Abeywardena, and J. S. Charnock. Dietary fat modulation of left ventricular ejection fraction in the marmoset due to enhanced filling. *Cardiovasc. Res.* **26**:871–877 (1992).

[3] J. S. Poling and M. A. Rogowski, unpublished observations.

Send reprint requests to: Stefano Vicini, Department of Physiology and Biophysics, Georgetown University Medical Center, 3900 Reservoir Road, Washington, DC 20007. Send email to: svicin01@gumedlib. dml. georgetown.edu